



Conjugation monitoring of gold nanoparticles with alkanedithiols by capillary zone electrophoresis

Toshio Takayanagi¹ · Koji Miyake² · Minamo Seto³ · Hitoshi Mizuguchi¹ · Hirotaka Okabe⁴ · Naoki Matsuda⁴

Received: 12 January 2023 / Accepted: 11 February 2023 / Published online: 21 February 2023
© The Author(s), under exclusive licence to The Japan Society for Analytical Chemistry 2023

Abstract

Alkanedithiols were used for the conjugation of gold nanoparticles (AuNP) prepared by a solution plasma process. Capillary zone electrophoresis was utilized for the monitoring of the conjugated AuNP. When 1,6-hexanedithiol (HDT) was used as a linker, a resolved peak from the AuNP was detected in the electropherogram; the resolved peak was attributed to the conjugated AuNP. The resolved peak was developed with increasing concentrations of HDT, while the peak of the AuNP decreased complementarily. The resolved peak also tended to develop along with the standing time at least up to 7 weeks. The electrophoretic mobility of the conjugated AuNP was almost identical over the HDT concentrations examined, suggesting that the conjugation of the AuNP did not proceed further, such as aggregate/agglomerate formation. The conjugation monitoring was also examined with some dithiols and monothiols. Resolved peak of the conjugated AuNP was also detected with 1,2-ethanedithiol and 2-aminoethanethiol.

Keywords Gold nanoparticles · Solution plasma process · Conjugation · Alkanedithiols · Capillary zone electrophoresis

Introduction

Gold nanoparticles (AuNP) are promising substance for the labeling and the detection of biogenic substances [1, 2]. When AuNP are used as a sensing material for target substances, it is essential for the AuNP to be dispersed in an aqueous solution, and various stabilizers have been developed [3]. Therefore, AuNP are also the analysis target on

physicochemical characterizations. In addition to traditional particle analyses, such as electron microscopy and dynamic light scattering, capillary zone electrophoresis (CZE) is also a useful analysis method for the dispersion monitoring of AuNP in an aqueous solution [4–6]. A broad peak has generally been detected with dispersed AuNP reflecting the wide variety of its size, shape, and charge; dispersion stability of AuNP in an aqueous solution have been evaluated through the broad peak [7–9]. Size resolutions of AuNP were also accomplished by CZE [10–13]. Since the number of charge of nanoparticles is proportional to the surface area of the nanoparticle, the electrophoretic mobility is theoretically proportional to the radius of the nanoparticle [13]. Morphology resolution and aspect ratio resolution were reported by CZE [14] and capillary transient isotachopheresis [15], respectively. The present authors also utilized CZE for the dispersion stability of AuNP prepared by a solution plasma (SP) process [16]. It was found that the AuNP stably dispersed in an aqueous solution for at least 55 weeks without any stabilizer [16]. Since the AuNP prepared by the SP process is stabilizer free [17–19], the AuNP is utilized as a surface-enhanced Raman scattering platform [18, 19].

Surface modification of AuNP has actively been investigated with thiols [20, 21] and biomolecules [22, 23]. AuNP

✉ Toshio Takayanagi
toshio.takayanagi@tokushima-u.ac.jp

✉ Naoki Matsuda
naoki.matsuda@aist.jp

¹ Graduate School of Technology, Industrial and Social Sciences, Tokushima University, 2-1 Minamijousanjima-cho, Tokushima 770-8506, Japan

² Graduate School of Science and Technology for Innovation, Tokushima University, 2-1 Minamijousanjima-cho, Tokushima 770-8506, Japan

³ Faculty of Science and Technology, Tokushima University, 2-1 Minamijousanjima-cho, Tokushima 770-8506, Japan

⁴ Sensing System Research Center, National Institute of Advanced Industrial Science and Technology, 807-1 Shukumachi, Tosu 841-0052, Japan

were sometimes conjugated or dimerized with modifiers of cetyltrimethylammonium bromide [24], amphiphilic polymer brushes [25], and biotin–avidin interactions [26]. When bifunctional substances such as dithiols are used for the modification of nanoparticle surface, the nanoparticles are sometimes conjugated. Silver nanoparticles were surrounded by much smaller AuNP with alkanedithiol linker forming heterogeneous core–satellite nanoassemblies [27]. Quantum dots of CdSe were linked with alkanedithiol forming hetero-assemblies [28]. Au nanorod–Au nanoparticle dimer structure was grown from the Au nanorod with the help of 4-mercaptophenol as a thiol ligand [29]. AuNP were also self-aggregated on silicon wafer surface by cross-linking with 1,6-hexanedithiol [30].

In this study, CZE was used for the monitoring of surface modification and/or conjugation of AuNP with alkanedithiols. By using CZE, the conjugated AuNP was electrophoretically resolved from the AuNP. The degree of the AuNP conjugation was considered from the changes in the electrophoretic mobility of the conjugated AuNP.

Experimental

Apparatus

An Agilent Technologies (Waldbronn, Germany) ^{3D}CZE equipped with a photodiode array detector was used as a CZE system. A fused silica capillary purchased from GL Sciences (Tokyo, Japan) was cut in an adequate length and it was packed in a cassette cartridge; the cartridge was installed in the CZE system. Dimensions of the separation capillary were 75 μm i.d., 375 μm o.d., 48.5 cm in total length, and 40 cm in effective length from the injection end to the detection point. A ChemStation software (Agilent Technologies, Ver. B04.02) was used for the control of the CE system, the data acquisition, and the data analysis. A Horiba (Kyoto, Japan) F-71 s pH meter was used for adjusting the pH of the separation buffers. A Transmission Electron Microscope (TEM) JEM-2100F (JEOL, Tokyo, Japan) was used for taking TEM images of the AuNP. The applied voltage of the electron gun was 200 kV, and the image resolution was 0.23 nm as the particle size.

Reagents

A separation buffer component of 2-[4-(2-hydroxyethyl)-1-piperazinyl]ethanesulfonic acid (HEPES) was purchased from Dojindo Laboratories (Kumamoto, Japan). Dithiol substances of 1,6-hexanedithiol (HDT) and 1,10-decanedithiol (DDT) were from FUJIFILM Wako Pure Chemical (Osaka, Japan). 2-Aminoethanethiol (AET), 2-mercaptoethanesulfonic acid sodium salt (MES), and 1-octadecanethiol

(ODT) were from Tokyo Chemical Industry (Tokyo, Japan). 1,2-Ethanedithiol (EDT) was from Nacalai Tesque (Kyoto, Japan). Other reagents were of analytical grade. Water used was purified by a Milli-Q Gradient A10 (Merck Millipore, Billerica, MA, USA).

An AuNP solution was prepared by an SP process as previously reported [16–19]. Namely, two Au electrodes were set with the angle of 30 degrees to the perpendicular direction into the SP reaction cell of a 50 mL Pyrex beaker, and the gap between the electrodes were kept at 0.5 mm. An aqueous solution of 5.0% (w/w) H_2O_2 was poured into the reaction cell. A high voltage bipolar pulsed power supply (MPS-06 K-01C, KURITA Seisakusho, Kyoto, Japan) was used as a power source. The applied bipolar voltage, the pulse width, and the frequency were 2.0 kV, 2.5 μsec , and 20 kHz, respectively. The energization period was set at 5 min. After preparing the AuNP solution, the AuNP solution was concentrated about fivefold by evaporating the solvent water by vacuum at ambient temperature. The AuNP thus prepared was conjugated with each thiol/dithiol substance as follows. An aliquot volume of 10 μL ethanol solution containing a thiol/dithiol was added to a 240 μL portion of the AuNP solution. The solution of the conjugated AuNP was stood for hours at ambient temperature, and the solution was subjected to the CZE analysis.

Procedure for the CZE measurements

A separation buffer was prepared with 10 mmol L^{-1} HEPES with its pH adjusted at 7.3 with NaOH. After the separation capillary being filled with the separation buffer, a conjugated AuNP solution was injected into the capillary from the anodic end by applying pressure of 50 mbar for 3 s. Both ends of the capillary were dipped in each buffer vial, and a DC voltage of 20 kV was applied to the capillary for the electrophoresis. The AuNP and the conjugated AuNP were photometrically detected at 250 nm. During CZE, the capillary cartridge was thermostat at 25 $^\circ\text{C}$ by circulating constant temperature air. Effective electrophoretic mobility (μ_{eff}) of the AuNP and the conjugated AuNP was calculated as in a usual manner using the migration times of the substance and the electroosmotic flow. The electroosmotic flow was monitored with ethanol added in the sample solution on the preparation of conjugated AuNP.

Results and discussion

Conjugation of AuNPs with 1,6-hexanedithiol

The AuNP prepared by the SP process is expected to be surface active [18, 19], and its reaction with the thiol/dithiol substances was aimed. Monothiol substances would simply

coat the surface of the AuNP, and therefore, the reaction with dithiols were examined in this study to link or conjugate the AuNP. First, HDT was chosen from the viewpoint of moderate carbon-chain length between two thiol moieties. The AuNP solutions after the addition of HDT were subjected to the CZE analysis. The results are shown in Fig. 1. As shown in Fig. 1a, a broad peak was detected with as-prepared AuNP. The AuNP itself is anionic, and it migrated slower than the electroosmotic flow (EOF) as in our previous study [16]. The broad peak suggests that the AuNP consists of wide variety of size and charge [7–9, 16]. Less shot signals in the electropherogram also suggest that the AuNP is well-dispersed in an aqueous solution [7–9, 16].

When HDT was added to the AuNP solution, another resolved peak from the AuNP was detected in the electropherograms as in Fig. 1c–g. Because HDT possesses two thiol moieties, plural AuNP would be linked or conjugated with HDT. The migration time of the resolved peak, conjugated AuNP, is shorter than that of as-prepared AuNP, and effective electrophoretic mobility of the conjugated AuNP is smaller than that of as-prepared AuNP. The electrophoretic mobility is proportional to the radius of nanoparticle [13], and the decrease in the effective electrophoretic mobility of the conjugated AuNP would be attributed to the decrease in the surface charge of the AuNP. Along with the increasing

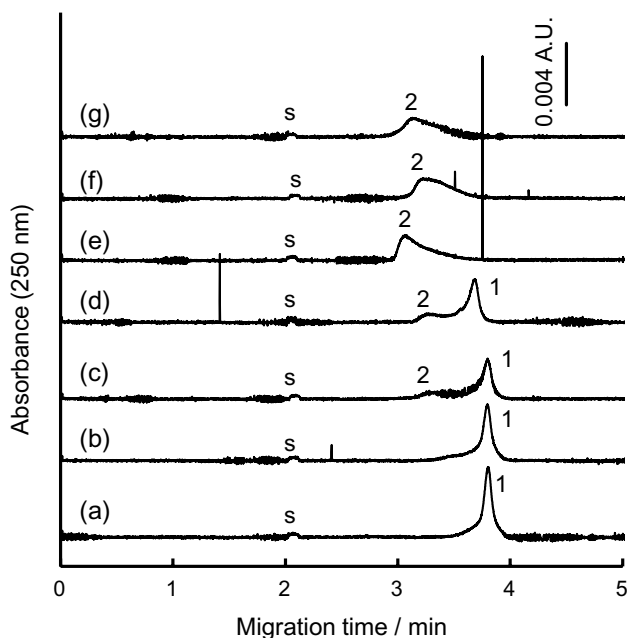


Fig. 1 Electropherograms of the AuNP after the reaction with 1,6-hexanedithiol (HDT). Peaks: 1, as-prepared AuNP; 2, conjugated AuNP with HDT. s: solvent (EOF). Concentration of HDT in the reaction vial: **a**, none; **b**, $1 \mu\text{mol L}^{-1}$; **c**, $2 \mu\text{mol L}^{-1}$; **d**, $3 \mu\text{mol L}^{-1}$; **e**, $5 \mu\text{mol L}^{-1}$; **f**, $10 \mu\text{mol L}^{-1}$; **g**, $20 \mu\text{mol L}^{-1}$. CZE conditions: 20 kV applied voltage, 250 nm detection wavelength, 25 °C capillary temperature, and 150 mbar*s sample injection

concentrations of HDT, the peak of as-prepared AuNP reduced and faded out. Corresponding to the reduction of the as-prepared AuNP peak, the resolved peak of the conjugated AuNP developed. The complementary relationship between two peaks of the AuNP species suggests that the conjugation of AuNP has been promoted with increasing concentrations of HDT. Because nanoparticles possess wide variation in size and shape, the reproducibility in both the migration time and the peak area in CZE is inferior to molecular ions [7, 16]. In addition, therefore, it was unavoidable that the total peak area attributed to the as-prepared AuNP and the conjugated AuNP was not steady. Less shot signals in the electropherograms also suggest the conjugation of the AuNP, i.e., early stage of the aggregation.

The conjugation of AuNP with HDT was evaluated through the effective electrophoretic mobility. The results are shown in Fig. 2. As-prepared AuNP, peak 1 in Fig. 1, showed almost identical electrophoretic mobility at around $3.5 \times 10^{-4} \text{ cm}^2 \text{ V}^{-1} \text{ s}^{-1}$. Similarly, the effective electrophoretic mobility of the resolved peak attributed to the conjugated AuNP showed almost a certain value over the HDT concentrations examined. The result suggests that the charge/mass ratio of the conjugated AuNP would be similar, and that the conjugation would not progress so much, such as aggregation/agglomeration.

Conjugation of AuNP with HDT was confirmed by TEM observations. Typical TEM images of AuNP are shown in Fig. 3. Characterization of the AuNP with its size and shape has been reported in our previous study. The average particle size was $20 \pm 14 \text{ nm}$ (mean \pm SD) [16], and the TEM image is cited in Fig. 3A [16]. TEM observation was done after the evaporation of the solvent, and aggregation/condensation of AuNP was not avoidable. However, the single particulate AuNP were observed with the as-prepared AuNP. On the other hand, conjugated AuNP, such as dimer and multimer,

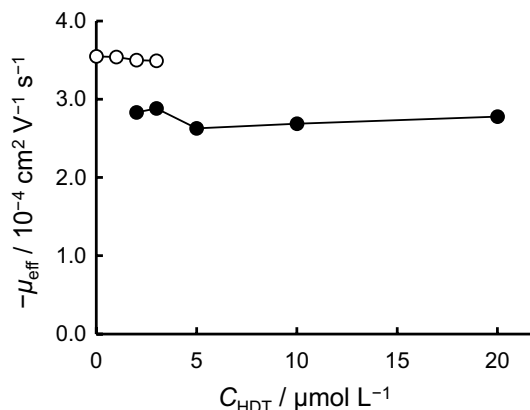


Fig. 2 Changes in the electrophoretic mobility of AuNP after the reaction with HDT. ○, as-prepared AuNP; ●, conjugated AuNP with HDT. CZE conditions are the same as in Fig. 1

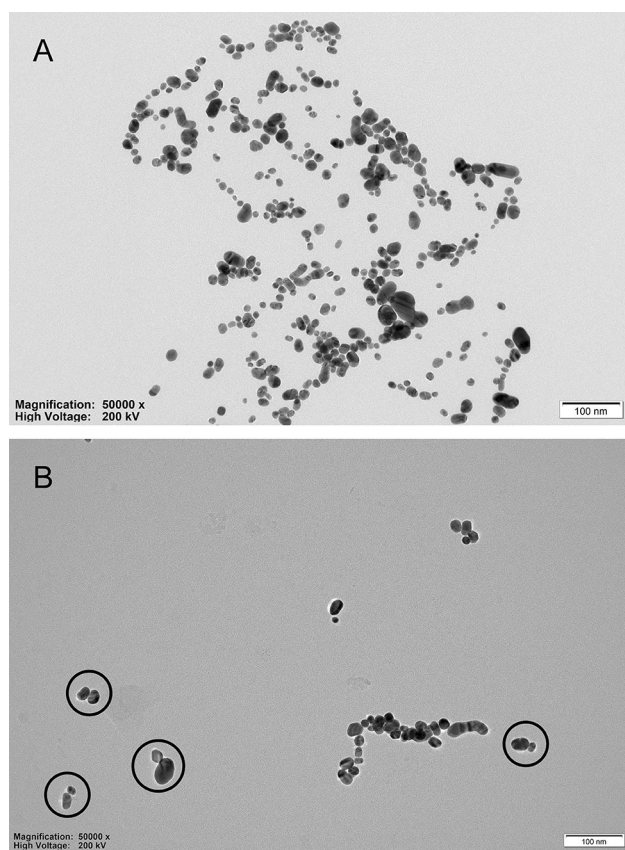


Fig. 3 TEM images of **A** as-prepared AuNP (cited from Ref. 16) and **B** conjugated AuNP with HDT. The grid mesh was covered with elastic wetty film for hydrophilization. Concentration of HDT in the AuNP solution B was $3 \mu\text{mol L}^{-1}$. The AuNP–HDT solution was diluted with an equal volume of ethanol. Dimerized AuNP are indicated with circles

were observed with HDT addition as shown in Fig. 3B. Dimerized AuNP suggest that two AuNP has been linked with bi-functional HDT. In addition, the fractions of dimer and multimer in TEM images increased at higher concentrations of HDT.

Long-term stability of the AuNP was examined with both as-prepared AuNP and the conjugated one. Two resolved peaks had been detected with the AuNP in the electropherograms at least over 7 weeks after the addition of $3 \mu\text{mol L}^{-1}$ HDT with less shot signals of the aggregates. In addition, the effective electrophoretic mobility of both as-prepared and the conjugated AuNP slightly changed (Supplementary Information, Fig. S1). The results suggest that the change in charge/mass ratio of the conjugated AuNP would be little, and the conjugation of the AuNP do not proceed further with the standing time. Meanwhile, the fraction of the peak area attributed to the conjugated AuNP (Peak 2) tended to develop against as-prepared AuNP (Peak 1) along with the storage time (Fig. 4). The result suggests that the conjugation of AuNP has further proceeded gradually. At the initial

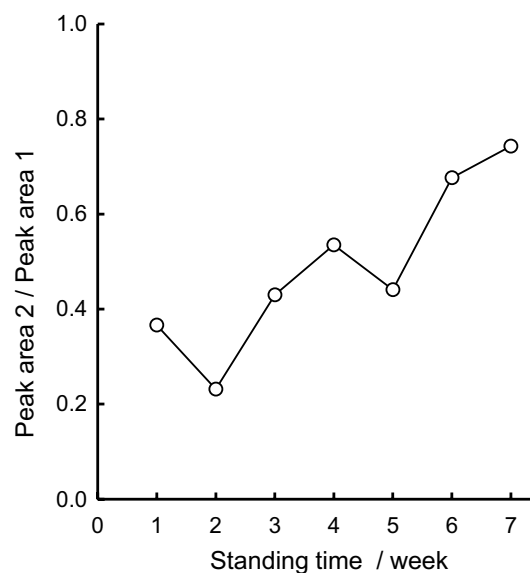


Fig. 4 Changes in the ratio of the peak area attributed to the conjugated AuNP (Peak 2 in Fig. 1) vs. as-prepared AuNP (Peak 1 in Fig. 1) over the storage period. Concentration of HDT was $3 \mu\text{mol L}^{-1}$. CZE conditions are the same as in Fig. 1

stage of the HDT addition, a portion of HDT would have modified the surface of as-prepared AuNP by reacting both ends of HDT on an AuNP. The HDT used for the surface modification of an AuNP may be transformed to the linking of two AuNP. As a result, the fraction of the conjugated AuNP increased with the standing time.

Conjugation of AuNPs with other dithiols

To examine the conjugation characteristics of the AuNP with HDT, a shorter dithiol substance of 1,2-ethanedithiol (EDT) was examined for comparison. Results are shown in Fig. 5. When EDT was added to the AuNP solution, conjugated AuNP was also detected as a resolved peak, as shown in Fig. 5b–e. The peak area of the resolved peak also developed with increasing concentrations of EDT, while the peak area of as-prepared AuNP reduced. A peak for the conjugated AuNP was detected over the EDT concentration at least up to 1 mmol L^{-1} without shot signals of the aggregation. Compared with the results in Fig. 1, the peak width of the conjugated AuNP with EDT is narrower. The result suggests that variation in size and charge of the conjugated AuNP would be smaller than the AuNP conjugated with HDT. Changes in the effective electrophoretic mobility are shown in Fig. 6. In contrast to HDT, the electrophoretic mobility of the conjugated AuNP reduced with increasing concentrations of EDT. The result suggests that the AuNP would further be conjugated with EDT. While the conjugated AuNP would contain several

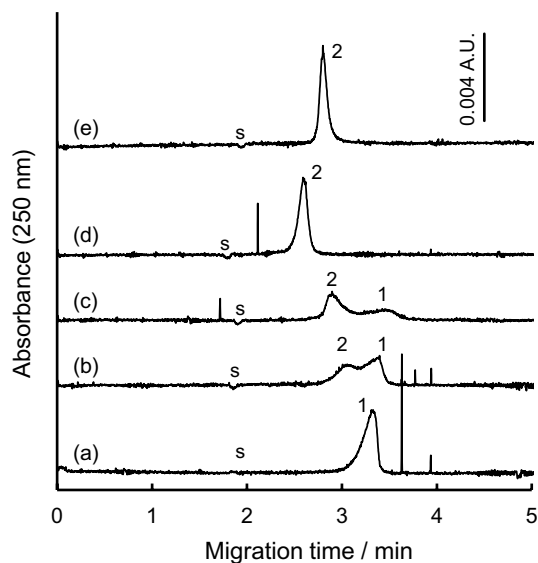


Fig. 5 Electropherograms of AuNP after the reaction with 1,2-ethanedithiol (EDT). Peaks: 1, As-prepared AuNP; 2, Conjugated AuNP with EDT. s: solvent (EOF). Concentration of EDT in the reaction vial: **a**, none; **b**, $3 \mu\text{mol L}^{-1}$; **c**, $5 \mu\text{mol L}^{-1}$; **d**, $10 \mu\text{mol L}^{-1}$; **e** $20 \mu\text{mol L}^{-1}$. CZE conditions are the same as in Fig. 1

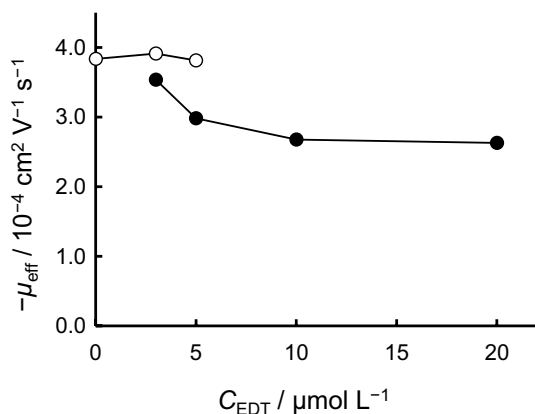


Fig. 6 Changes in the electrophoretic mobility of AuNP after the reaction with EDT. ○, As-prepared AuNP; ●, Conjugated AuNP. CZE conditions are the same as in Fig. 1

conjugation species, a single peak is detected with the conjugated AuNP and resolution among the conjugated species would be difficult.

Another dithiol substance of 1,10-decanedithiol (DDT) was also examined as a long-chained one. Results are shown in Fig. S2 (Supplementary Information). Any resolved peak from the AuNP was not detected with DDT but fronting from the as-prepared AuNP was observed. Changes in the electrophoretic mobility from as-prepared AuNP to the conjugated AuNP would not be sufficient to resolve them.

Binding of AuNPs with monothiools

Monothiol substances were also examined for the comparison with the dithiols. Monothiol substances examined were nonionic and hydrophobic 1-octadecanethiol (ODT), anionic 2-mercaptoethanesulfonate ion (MES), and cationic 2-aminoethanethiol (AET). Anionic thiols of mercaptodecanoic acid [31] and 3-mercapto-1-propanesulfonate [32] were used for the stabilization of AuNP in an aqueous solution by forming self-assembled monolayer. Electropherograms are shown in Fig. S3 (Supplementary Information), Fig. S4 (Supplementary Information) and Fig. 7, respectively. When the AuNP was reacted with ODT, any resolved peak was not detected (Fig. S3). It would be because ODT is monothiol and it does not link plural AuNP. The effective electrophoretic mobility gradually decreased along with the addition of ODT. ODT simply covered and modified the AuNP surface, and degree of the charge/mass ratio of the ODT-modified AuNP would have decreased. Serious shot signals were not detected, and the ODT-modified AuNP would not be aggregated by the reaction with ODT. When MES was used as a surface modifier, single peak was also detected with as-prepared AuNP and/or the surface-modified AuNP (Fig. S4). Since MES is anionic, decrease in the effective electrophoretic mobility was smaller with the MES-modified AuNP; changes in the charge/mass ratio would be little. The little change in charge/mass ratio did not allow the CZE resolution between as-prepared and the surface-modified AuNP.

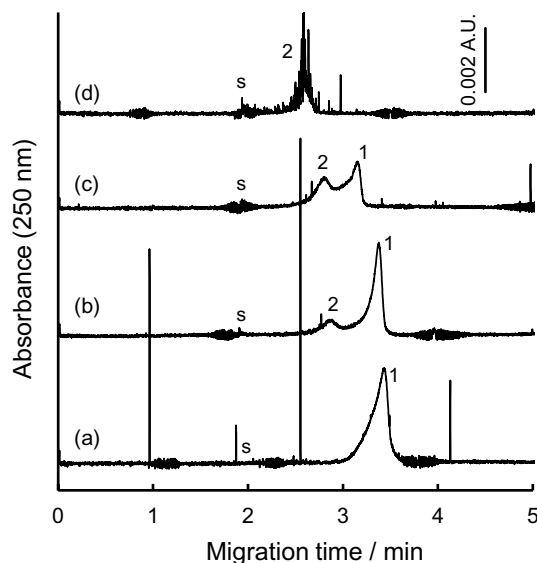


Fig. 7 Electropherograms of AuNP after the reaction with 2-aminoethanethiol (AET). Peaks: 1, AuNP; 2 Conjugated AuNP with AET. s: solvent (EOF). Concentration of AET in the reaction vial: **a**, none; **b**, $1 \mu\text{mol L}^{-1}$; **c**, $2 \mu\text{mol L}^{-1}$; **d**, $3 \mu\text{mol L}^{-1}$. CZE conditions are the same as in Fig. 1

On the other hand, a resolved peak was detected with the AET-modified AuNP as shown in Fig. 7. Two reasons can be assumed with the resolved peak with AET. One is the bi-functional character of AET; AET could linked plural AuNP. The other is the cationic character of AET; the electrophoretic mobility of the AuNP would sufficiently be decreased by the surface coating. Serious shot signals were detected with the resolved peak as in Fig. 7d, and agglomeration of AuNP would have been promoted with AET. Agglomeration is generally induced with the decrease in the surface charge of AuNP, and cationic character of AET would be applied to this resolved peak. Modification with cationic AET would decrease the anionic charge of the AuNP, and dispersity of the AuNP by the electrostatic repulsion would have reduced by the modification. Changes in the charge/mass ratio, as well as the effective electrophoretic mobility, would be sufficient to resolve AET-modified AuNP from the as-prepared AuNP. Peak area attributed to the AET-modified AuNP increased with increasing concentrations of AET added in the AuNP solution, and peak area for the as-prepared AuNP decreased complementary.

Conclusions

In this study, a resolved peak was detected with conjugated AuNP with the alkanedithiols of HDT and EDT based on the changes in the charge/mass ratio of the conjugates. Degree of the conjugation is simply estimated through the peak area between as-prepared AuNP and the conjugated AuNP. The dispersion stability of the conjugates can also be evaluated through the absent detection of shot signals. It is demonstrated in this study that CZE would be a useful and conventional characterization method for the conjugation monitoring of AuNP through the electrophoretic separation and the electrophoretic mobility.

Supplementary Information The online version contains supplementary material available at <https://doi.org/10.1007/s44211-023-00299-4>.

Acknowledgements This work was supported in part by Japan Society for the Promotion of Sciences (JSPS) KAKENHI Grant Number 20K05568. The authors acknowledge to Mr. Tomoyuki Ueki (Tokushima University) for the TEM measurements.

Data availability The data sets generated during and/or analyzed during the current study are available from the corresponding author on reasonable request.

Declarations

Conflict of interest The authors declare that they have no conflict of interest.

References

1. L. Qin, G. Zeng, C. Lai, D. Huang, P. Xu, C. Zhang, M. Cheng, X. Liu, S. Liu, B. Li, H. Yi, *Coordin. Chem. Rev.* (2018). <https://doi.org/10.1016/j.ccr.2018.01.006>
2. C. Kokkinos, *Nanomaterials* (2019). <https://doi.org/10.3390/nano9101361>
3. J.W. Krumpfer, T. Schuster, M. Klapper, K. Müllen, *Nano Today* (2013). <https://doi.org/10.1016/j.nantod.2013.07.006>
4. F.-K. Liu, *J. Chromatogr. A.* (2009). <https://doi.org/10.1016/j.chroma.2009.07.026>
5. U. Pyell, *Electrophoresis* (2010). <https://doi.org/10.1002/elps.200900555>
6. V. Adam, M. Vaculovicova, *Electrophoresis* (2017). <https://doi.org/10.1002/elps.201700097>
7. A. Pallotta, A. Boudier, P. Leroy, I. Clarot, *J. Chromatogr. A.* (2016). <https://doi.org/10.1016/j.chroma.2016.07.031>
8. S. Dziomba, K. Ciura, P. Kocialkowska, A. Prah, B. Wielgomas, *J. Chromatogr. A.* (2018). <https://doi.org/10.1016/j.chroma.2018.03.038>
9. S. Dziomba, K. Ciura, B. Correia, B. Wielgomas, *Anal. Chim. Acta.* (2019). <https://doi.org/10.1016/j.aca.2018.09.069>
10. W.-M. Hwang, C.-Y. Lee, D.-W. Boo, J.-G. Choi, *Bull. Kor. Chem. Soc.* (2003). <https://doi.org/10.5012/bkcs.2003.24.5.684>
11. F.-K. Liu, Y.-Y. Lin, C.-H. Wu, *Anal. Chim. Acta.* (2005). <https://doi.org/10.1016/j.aca.2004.08.052>
12. R. Ciriello, P.T. Iallore, A. Laurita, A. Guerrieri, *Electrophoresis* (2017). <https://doi.org/10.1002/elps.201600478>
13. H. Qu, T.K. Mudalige, S.W. Linder, *Anal. Chem.* (2014). <https://doi.org/10.1021/ac5025655>
14. C. Adelantado, M. Algarra, M. Zougagh, Á. Ríos, *Electrophoresis* (2018). <https://doi.org/10.1002/elps.201800035>
15. K.R. Riley, H. El Hadri, J. Tan, V.A. Hackley, W.A. MacCrehan, *J. Chromatogr. A.* (2019). <https://doi.org/10.1016/j.chroma.2019.03.054>
16. T. Takayanagi, K. Miyake, S. Iwasaki, D. Uehara, H. Mizuguchi, H. Okabe, N. Matsuda, *Anal. Sci.* (2022). <https://doi.org/10.1007/s44211-022-00149-9>
17. N. Matsuda, T. Nakashima, *IEICE Tech Rep.* (2012) (No doi) <https://ken.ieice.org/ken/paper/20120217000z/eng/>. Accessed 12 Jan 2023
18. N. Matsuda, T. Nakashima, H. Okabe, H. Yamada, H. Shiroishi, T. Nagamura, *Mol. Cryst. Liq. Cryst.* (2017). <https://doi.org/10.1080/15421406.2017.1351269>
19. N. Matsuda, H. Okabe, T. Nagamura, M. Uehara, *Mol. Cryst. Liq. Cryst.* (2019). <https://doi.org/10.1080/15421406.2019.1648038>
20. C. Vericat, M.E. Vela, G. Benitez, P. Carro, R.C. Salvarezza, *Chem. Soc. Rev.* (2010). <https://doi.org/10.1039/B907301A>
21. J. Li, B. Zhu, X. Yao, Y. Zhang, Z. Zhu, S. Tu, S. Jia, R. Liu, H. Kang, C.J. Yang, *ACS Appl. Mater. Interfaces.* (2014). <https://doi.org/10.1021/am504139d>
22. S. Su, X. Zuo, D. Pan, H. Pei, L. Wang, C. Fan, W. Huang, *Nanoscale* (2013). <https://doi.org/10.1039/c3nr33870c>
23. A.E. James, J.D. Driskell, *Analyst.* (2013). <https://doi.org/10.1039/C2AN36467K>
24. Y. Cen, X. Huang, R. Zhang, J.-Y. Chen, *J. Fluoresc.* (2014). <https://doi.org/10.1007/s10895-014-1433-9>
25. L. Cheng, J. Song, J. Yin, H. Duan, *J. Phys. Chem. Lett.* (2011). <https://doi.org/10.1021/jz201011b>
26. Y. Lyu, Á. Martínez, F. D'Inca, F. Mancini, P. Scrimin, *Nanomaterials* (2021). <https://doi.org/10.3390/nano11061559>
27. J.H. Yoon, Y. Zhou, M.G. Blaber, G.C. Schatz, S. Yoon, *J. Phys. Chem. Lett.* (2013). <https://doi.org/10.1021/jz400602f>
28. C.N. Dibenedetto, E. Fanizza, L. De Caro, R. Brescia, A. Pannello, R. Tommasi, C. Ingrassio, C. Giannini, A. Agostiano, M.L.

- Curri, M. Striccoli, *Mater. Res. Bull.* (2022). <https://doi.org/10.1016/j.materresbull.2021.111578>
29. J. Huang, Y. Zhu, C. Liu, Z. Shi, A. Fratolocchi, Y. Han, *Nano Lett.* (2016). <https://doi.org/10.1021/acs.nanolett.5b04329>
30. M. Stetsenko, T. Margitych, S. Kryvyi, L. Maksimenko, A. Hassan, S. Filonenko, B. Li, J. Qu, E. Scheer, S. Snegir, *Nanomaterials* (2020). <https://doi.org/10.3390/nano10030512>
31. T. Laaksonen, P. Ahonen, C. Johans, K. Kontturi, *Chem. Phys. Chem.* (2006). <https://doi.org/10.1002/cphc.200600307>
32. L. Carlini, C. Fasolato, P. Postorino, I. Fratoddi, I. Venditti, G. Testa, C. Battocchio, *Colloids Surf. A.* (2017). <https://doi.org/10.1016/j.colsurfa.2017.05.045>

Springer Nature or its licensor (e.g. a society or other partner) holds exclusive rights to this article under a publishing agreement with the author(s) or other rightsholder(s); author self-archiving of the accepted manuscript version of this article is solely governed by the terms of such publishing agreement and applicable law.